Available online at www.sciencedirect.com

ScienceDirect

Procedia Engineering 147 (2016) 168 – 174

Procedia Engineering

www.elsevier.com/locate/procedia

11th conference of the International Sports Engineering Association, ISEA 2016

Musculoskeletal modelling of elite handcycling motion: evaluation of muscular on- and offset

Eduard-Max Felsner[a], Stefan Litzenberger[a,b,*], Franziska Mally[a,b], Anton Sabo[a,b]

[a]*Institute for Biomedical, Health and Sports Engineering, University of Applied Sciences Technikum Wien, 1200 Vienna, Austria*
[b]*School of Aerospace, Mechanical and Manufacturing Engineering, RMIT University, Melbourne, VIC 3083, Australia*

Abstract

Handcycling, as a competitive sport, has been a Paralympic discipline since 2004 and is performed by handicapped athletes with impairments of the spine or brain. In this work a musculoskeletal model of a handcyclist is developed in the software AnyBody using kinematic data from a previous study of handcycling of one male elite handbiker (class: H3.2). The on- and offset timing of several muscles of the upper body (left and right of: m. pectoralis, m. deltoideus, m. biceps brachii and m. triceps brachii) were calculated with different thresholds and compared to results from surface electromyography (sEMG) measurements recorded during the previously mentioned subject study. It could be shown, that the mean overlap of muscle activation times was between a satisfying 64% and 75% depending on the threshold used. However, especially for m. deltoideus a very different on- offset behaviour was observed in the simulation than in the sEMG measurements resulting from the positioning of the electrodes in the subject study on one specific branch of the m. deltoideus and insufficient knowledge about the actual course of the crank torque for this specific athlete. Thus given sufficient accuracy of input parameters - musculoskeletal modelling could be used to predict changes in muscle activity timing for different handcycle setups.

Peer-review under responsibility of the organizing committee of ISEA 2016

Keywords: handcycling, muscular timing, sEMG, musculoskeletal simulation

1. Introduction

Handcycling has been a Paralympic discipline since 2004 and is performed by athletes with impairments of the spine or brain. The propulsion of the front wheel results from a synchronous movement of two cranks turned by the athletes arms that is transmitted via a chain. Due to the similarity of the mechanical propulsion system, handcycling parameters are comparable to bicycle parameters. However, in contrast to bicycling there has been little research in handcycling in terms of parameters like sitting position, backrest height and crank height and length.

The main focus of previous research was on the effect of crank length and cadence on the power output [1], the differences between synchronous and asynchronous propulsion technique [2] and the influence of the backrest on

* Corresponding author. Tel.: +43-1-3334077-377 ; fax: +43-1-3334077-99377.
E-mail address: stefan.litzenberger@technikum-wien.at

Peer-review under responsibility of the organizing committee of ISEA 2016
doi:10.1016/j.proeng.2016.06.208

the power output [3]. The influence of crank length, crank height and backrest height on muscular activities and kinematics were investigated for one elite athlete [4].

Musculoskeletal modelling has been used for the optimization of many parameters of human motion and sports equipment. De Jong et al.[5] used a musculoskeletal model to optimize seat height and distance as well as cadence for recumbent cycling. Holmberg and Lund[6] investigated the influence of different techniques in cross country skiing and Dubowsky et al.[7] used the approach in a medical application to minimize shoulder joint forces during wheelchair-propulsion.

Whereas subject-studies always underlie a bias by the experience of subjects with standard parameters and lacking experience with new parameters. This can influence motion patterns, coordination and therefore measurement results. The solution to avoid those drawbacks can be musculoskeletal modelling. Musculoskeletal modelling has already been used to predict muscle forces under different settings, to perform motion optimization studies or to compare different algorithms [6,8–13].

The simulation of muscle activities has several advantages. Compared to experimental tests a validated musculoskeletal model is reproducible and independent from subjects. In case the simulation delivers promising results, the investigated parameters can be changed in real-life applications and tested experimentally.
The main reason why muscular activity is taken for the validation of the model is that it is easy to measure in comparison to other parameters. Compared to muscle-force or joint-moments, where special measuring equipment is needed for every motion, sEMG-electrodes can be easily placed on the muscles for almost all sportive motions.

In this study, an algorithm published in [14] is used for the computation of muscle activities of a motion capture driven handcycling model. The simulated muscle activities are compared to via EMG measured activities to validate the model. It was expected, that simulated muscular activity, in terms of muscular timing (i.e. on- and offset times of the muscles) is comparable to experimentally acquired data.

2. Methods and materials

The musculoskeletal modelling was done in the software AnyBody 6.0.5 (AnyBody Technology, Aalborg, DEN) by adapting the basic model *MoCapModel* from the AnyBody Managed Model Repository 1.6.3 (AMMR), for data analysis Matlab (V 7.11.0.548, The Mathworks Inc., Natick, USA) was used. The model is mainly driven by motion capture data, acquired in a previous study [4]. Some drivers had to be added in order to fix the model to the coordinate system and the modeled handbike.

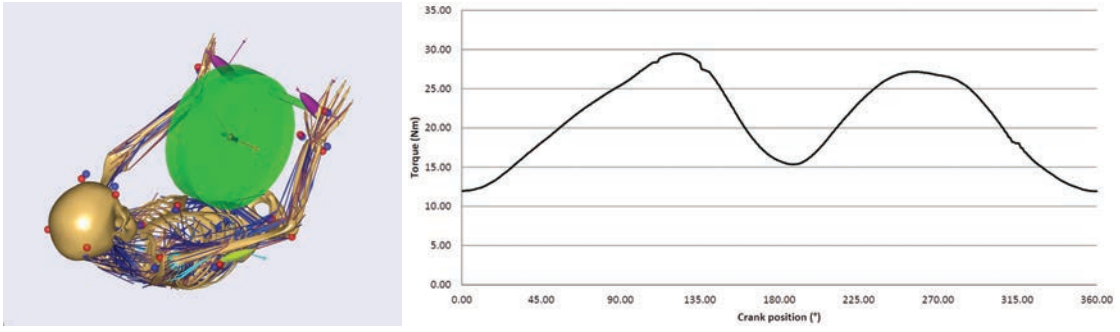

(a) (b)

Fig. 1. (a) Musculoskeletal model of the handbiker including the environment, (b) Mean torque distribution over a crank-cycle (source:(b) [15]).

The AnyBody study consists of two sub-studies. The first study is a kinematic analysis that loads motion capture data from the c3d-file and optimizes marker positions and segment lengths according to the subjects segment lengths. From this study interpolation drivers are calculated which are used to drive the model in the inverse dynamic study, which is the second sub-study. The inverse dynamic study contains an environment including a handbike consisting of a frame, which is connected to the coordinate system, a crank and two handles, which are the connection between

Table 1. Overview of used trials and different settings; crank position (c-pos): 1 = lowest, 4 = highest; backrest height (back-h): lo = low, hi = high; crank length (c-len); power level (P).

	T1-130	T1-160	T1-190	T2	T3
c-pos	2	2	2	4	1
back-h	lo	lo	lo	lo	hi
c-len [mm]	165	165	165	165	175
P [W]	130	160	190	160	190

model and environment (Figure 1a). Due to missing coordinates of the pivot point of the crank, the coordinates had to be approximated from the motion capture data of the finger markers, placed on the head of the second metacarpal.

As the torque distribution was not measured during the initial study [4], a torque distribution from literature [15] is applied (Figure 1b). The measured mean torque was fitted into the torque distribution with Matlab's curve fitting tool and implemented as an equation, where the point of origin of the load was defined as the pivot point of the crank.

For the validation of the model, the activities of m. pectoralis (PECT), m. deltoideus (DELT), m. biceps brachii (BIC) and m. triceps brachii (TRIC) of both sides are investigated and compared to the measured activities from the initial study [4]. As most of the muscles in this model consist of several parts (e.g. m. biceps brachii: long and short head), all these parts from the model are summed within each muscle for the comparison with sEMG data.

For the validation, five different trials with different settings were investigated. The variable parameters were the power level, the crank-height, crank-length and the height of the backrest (Table 1). Three trials with equal positions and different power levels were chosen to investigate the influence of the power level on the muscular activity (T1-130, T1-160, T1-190). The other two trials represent two extreme positions. One with a large distance between the shoulder and the most forward position of the crank due to highest possible crank position (T2) and one with a short distance between shoulder and the most forward position due to the lowest possible crank height, a high backrest and a longer crank (T3).

In order to compare simulated and measured muscular activities, the results of both are normalized to one mean crank cycle (i.e.360°) and on-off timing is calculated for each muscle. In the in-situ measurements a muscle is defined as *on* when its activity reaches a threshold ≥ 30% of the difference between maximum and minimum activity. As defined thresholds can influence the results [5], four different thresholds (10% (TH10), 20% (TH20), 25% (TH25) and 30% (TH30) of the maximum muscle activity occurring during the mean crank-cycle) are applied to the simulation data to identify the best threshold for this model. In order to quantify the results, the mean overlap duration in percent between the simulated and measured *on*-times is calculated using (1). In total there are 360 data-points representing every single degree of crank-position. t_{both} is the sum of data-points the muscle is *on* in both - simulation and measurement - concurrently. t_s and t_m signify the sums of data-points the muscle is *on* in the simulation and measurements, respectively. The mean overlap describes the percentage of the duration the muscle is active in both measurement and simulation.

$$Overlap[\%] = \frac{t_{both}}{\frac{t_s+t_m}{2}} \cdot 100 \tag{1}$$

3. Results

Table 2 shows the influence of the threshold on the results by comparing the mean overlap of activation times for four different thresholds and the mean of three muscles. The overlap of DELT-activation times is not included in this table due to doubtful results that will be discussed in section 4.

The largest overlap (69% to 75%) is achieved for the simulation of T2. T1-160 shows the smallest overlap (64% to 66%). A higher overlap signifies a better match between simulated and measured data. For different trials, however, different thresholds displayed the best results, indicating that not one single threshold could be regarded as best. TH10 has the largest overlap for T2, T3 and T1-160 at TH20, whereas TH20 shows the best result for T1-130, and TH25 is the best threshold for T1-190.

Table 3 shows the overlap of activation times for all four muscles and all five trials with the threshold TH20. The best overlap in all five trials was achieved for PECT (81.93%–92.96%). The overlap of DELT is the lowest with values

Table 2. Mean overlap of activation times [%] between measured and simulated muscle activities for four thresholds (TH10, TH20, TH25 and TH30) and three muscles (mean(PECT, BIC, TRIC)).

	TH10	TH20	TH25	TH30
T1-130	67±14	69±16	68±19	68±23
T1-160	66±15	66±19	66±20	64±21
T1-190	67±16	67±18	68±20	67±21
T2	75±15	71±19	70±20	69±22
T3	69±14	67±15	66±18	66±20

Table 3. Overlap of activation times [%] between measured and simulated muscle activities for four muscles (PECT, DELT, BIC and TRIC) of both sides (Left and Right) and five trials (T1-130/160/190, T2 and T3) with mean value and standard deviation for the threshold TH20.

	T1-130	T1-160	T1-190	T2	T3
PECT L	89.31	86.77	90.46	90.74	92.96
PECT R	87.09	90.58	84.92	81.93	85.18
DELT L	17.63	13.67	19	0	9.7
DELT R	10.47	16.79	0	40.71	28.57
BIC L	67.12	56.13	58.54	57.05	70.51
BIC R	63.24	62.55	64.91	59.91	80.63
TRIC L	49.28	46.38	45.05	54.59	45.88
TRIC R	57.73	52.46	55.84	57.63	50.56
MEAN±SD	55±29	53±28	52±31	55±27	58±29

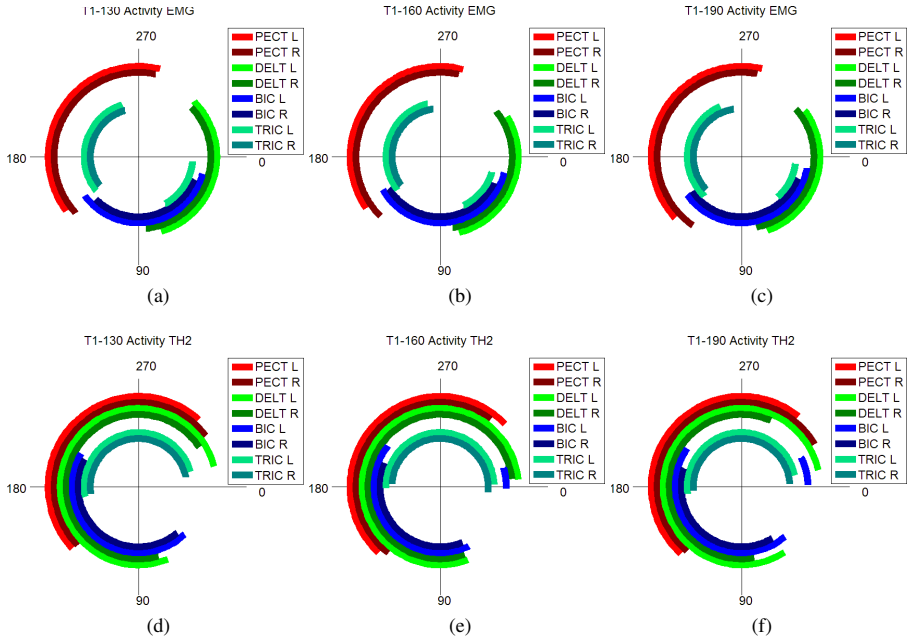

Fig. 2. Mean activation times of all investigated muscles during one crank cycle for the trials (a),(d) 1-130, (b),(e) T1-160 and (c),(f)T1-190; (a),(b),(c) measured sEMG data; (d),(e),(f) simulated data for threshold TH20

from 0% to 40.71%. These results show that the simulated muscular activity of PECT matches with the measured one quite well. The reason for the poor overlap of the DELT will be addressed in the Discussion.

The activation times of the four muscles in the mean crank cycle are shown in (Figure 2). For the trial T1-130 (Figure 2a,2d) the biggest differences can be observed for DELT. In the measurement (Figure 2a) DELT is active between approximately 310° and 80° whereas in the simulation (Figure 2d) it is active between approximately 80°

and 330° which is the completely opposite region in the crank cycle. The biggest overlap can be observed for PECT, which is active between approximately 135° and 280° in the measurements and between approximately 135° and 320° in the simulation. A noticeable shift of the activation time from BIC can be observed. In the measurements BIC is mostly active in the first quarter of the crank cycle, whereas it is mostly active in the second quarter in the simulation. Nearly the same shift can be observed for TRIC. Another noticeable fact is a second activity of TRIC in the first quarter of the crank cycle during the measurements, which does not occur during the simulation. The only remarkable difference from T1-130 (Figure 2a, 2d) to T1-160 (Figure 2b, 2e) is an additional activity of BIC just before 0° during the simulation of T1-160. The most noticeable difference between T1-190 (Figure 2c, 2f) and the before mentioned trials are the bigger differences between left and right side that occur in the measurements as well as in the simulations. In Figure 3 the mean activation of the trials T2 (Figure 3a3b) and T3 (Figure 3c3d) can be

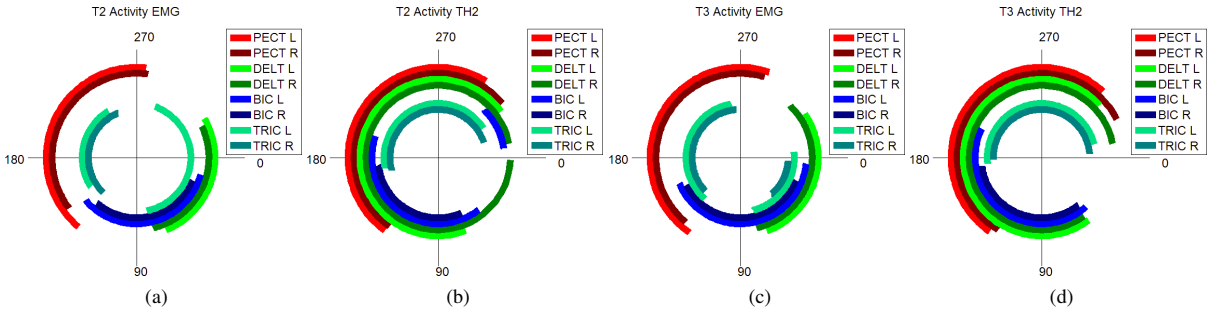

Fig. 3. Mean activation times of all investigated muscles during one crank cycle for the trials (a),(b) T2 and (c),(d) T3; (a),(c) measured sEMG data; (b),(d) simulated data for threshold TH20.

seen. The activation times for T2 show a long second period of activity for the left TRIC during the measurement (Figure 3a). However, this second period does not occur during the simulation (Figure 3b). The same behavior can be observed for T3 (Figure 3c3d). In T3, also the right TRIC has a second period of activity during the measurements (Figure 3c). Apart from that, activation times of T2 and T3 (Figure 3)show similar results to the activation times of T1-130/160/190 (Figure 2).

4. Discussion and conclusion

The overlap of muscle activation times show values between 64% and 75% depending on the investigated trial and the used threshold. No best threshold value can be observed for all the results. However, the most promising results can be achieved with thresholds of 10% (TH10) and 20% (TH20) of maximum muscular activity. The fact that different threshold show best results for different trials leads to the assumption that the optimum threshold is an individual optimum threshold for each trial, but also that the optimum threshold is in the range between 10% and 20% of maximum activity. These results correspond to those of [5], who discovered a threshold of 20% to be the most accurate for their study. All in all, a mean overlap between 64% and 75% is satisfying to validate the model in terms of investigated parameters. The most remarkable difference between in-situ measured activation times and simulated activation times is the shift of BIC and TRIC in all five trials and for both sides which is induced by the torque distribution adapted from [15]. For this torque data the maxima occur at 135° and 270° which corresponds exactly to the activation of BIC and TRIC in the simulation. At the same time in the measurements, BIC and TRIC are at the end of their activity or not even active which leads to a lower overlap of activation times for these two muscles. PECT is far less affected by the torque and therefore very accurate in terms of overlap.

Comparing the measured activation times of DELT to the simulated activation times it can be noticed, that DELT is active in complete opposite parts of the mean crank cycle for all trials (Figure 2,3). The most likely reason for these results is the high complexity of anatomy and physiology of DELT and the placement of the sEMG-electrodes. In the simulation the DELT is split into twelve parts (six scapular, six clavicular). For the comparison, the activity of all these parts is summed to total activity of DELT. Due to the big surface of DELT, the electrodes can just record the signal of a small area corresponding approximately to the scapular parts 2-4 in the simulation.

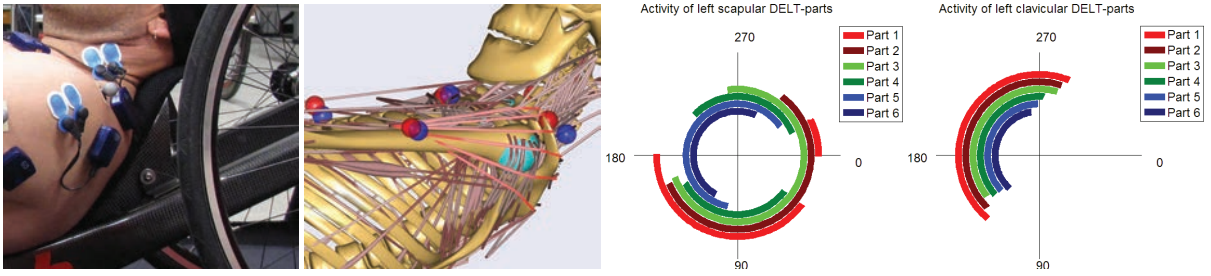

Fig. 4. Comparison between the placements of the electrodes in the in-situ study and the modeled anatomy in the simulation. (a) Point of attachment of the electrodes on the DELT in the in-situ measurement (REF); (b) modeled anatomy of the DELT with the 6 red highlighted scapular parts from 1=lowest to 6=highest; (c), (d) Activities of all parts of left DELT for the trial T1-190: (c) scapular parts, (d) clavicular parts

Figure 4c and 4d show the activation times in the mean crank cycle of all twelve parts of the left DELT for the trial T1-190. It can be noticed that the scapular parts 2-4 (Figure 4c) show activity in the first and last quarter of the mean crank cycle, whereas the scapular parts 5 and 6 and also the clavicular parts 1-6 show activity in the second and third quarter of the mean crank cycle. Summing all twelve parts of the simulation to one activity leads to the result, that DELT is active in the second and third quarter of the crank cycle. The activities of the scapular parts 2-4 correspond to the results of the in-situ measurements, where DELT is active in the first and last quarter. These parts of DELT mainly have the function of abduction of the humerus which takes place between 315° and 80° of the crank cycle, which corresponds to the findings of [16]. The parts that seem to generate a higher activity are responsible for the anteversion and retroversion of the humerus. These parts are the scapular parts 5 and 6 (Figure 4c) as well as clavicular parts 1-6 (Figure 4d). As a conclusion it can be said, that summing the activity of all parts of a muscle is not the best method for comparing complex muscles like DELT.

In conclusion it can be stated, that the model corresponds to the measured data for most of the muscles in terms of activation times (muscular on- and offset). The results are promising, but could definitely be improved by more accurate input data (e.g. the real torque distribution of this specific subject). The method of summing activities of several parts of a muscle for the comparison with measured data proved to be useful for simple muscles with simple functionality like BIC, TRIC and PECT. However, for more complex muscles like DELT it turned out to deliver doubtful results that can be explained by observing the activity of single parts of such muscles.

Nevertheless a functioning model of handcyling based on motion capture data was established. Like in other studies [5–7] this model can be used to optimize parameters of handcycling in terms of equipment and motion.

References

[1] V. L. Goosey-Tolfrey, H. Alfano, N. Fowler, The influence of crank length and cadence on mechanical efficiency in hand cycling, European journal of applied physiology 102 (2008) 189–194.

[2] L. H. van der Woude, A. Horstman, P. Faas, S. Mechielsen, H. A. Bafghi, J. J. de Koning, Power output and metabolic cost of synchronous and asynchronous submaximal and peak level hand cycling on a motor driven treadmill in able-bodied male subjects, Medical engineering & physics 30 (2008) 574–580.

[3] A. Faupin, P. Gorce, C. Meyer, A. Thevenon, Effects of backrest positioning and gear ratio on nondisabled subjects' handcycling sprinting performance and kinematics, Journal of rehabilitation research and development 45 (2008) 109.

[4] S. Litzenberger, F. Mally, A. Sabo, Influence of different seating and crank positions on muscular activity in elite handcycling-a case study, Procedia Engineering 112 (2015) 355–360.

[5] P. De Jong, M. De Zee, P. Hilbers, H. Savelberg, F. van de Vosse, A. Wagemakers, K. Meijer, Multi-body modelling of recumbent cycling: an optimisation of configuration and cadence, Master's Thesis Medical Engineering, TU/e Biomodelling and Bioinformatics, University of Maastricht, Movement Sciences, Aalborg University (2006).

[6] L. J. Holmberg, A. M. Lund, A musculoskeletal full-body simulation of cross-country skiing, Proceedings of the Institution of Mechanical Engineers, Part P: Journal of Sports Engineering and Technology 222 (2008) 11–22.

[7] S. R. Dubowsky, J. Rasmussen, S. A. Sisto, N. A. Langrana, Validation of a musculoskeletal model of wheelchair propulsion and its application to minimizing shoulder joint forces, Journal of Biomechanics 41 (2008) 2981–2988.

[8] Y. Collet, P. Tétreault, J. Rasmussen, N. Nuño, N. Hagemeister, Computational modeling of a prosthetic shoulder: our experience with the anybody modeling system, in: Proceedings of the IASTED International Conference on Modelling and Simulation, 2007, pp. 624–9.
[9] Y. Jung, M. Jung, K. Lee, S. Koo, Ground reaction force estimation using musculoskeletal simulation, in: ISBS-Conference Proceedings Archive, volume 1, 2012.
[10] K. Prajapati, F. Barez, J. Kao, D. Wagner, Dynamic force response of human legs due to vertical jumps, in: ASME 2011 International Mechanical Engineering Congress and Exposition, American Society of Mechanical Engineers, 2011, pp. 1–8.
[11] J. Rasmussen, L. J. Holmberg, K. Sørensen, M. Kwan, M. S. Andersen, M. de Zee, Performance optimization by musculoskeletal simulation, Movement & Sport Sciences 75 (2012) 73–83.
[12] S. Chen, M. S. Andersen, J. Rasmussen, W. Tang, The effect of muscle setting on kinetics of upper extremity in a baseball pitching modeling: A case study, in: ISBS-Conference Proceedings Archive, volume 1, 2013.
[13] N. Petrone, D. Tregnaghi, M. Nardon, G. Marcolin, Musculoskeletal simulation of isokinetic exercises: A biomechanical and electromyographical pilot study, Procedia Engineering 112 (2015) 250 – 255. 'The Impact of Technology on Sport VI' 7th Asia-Pacific Congress on Sports Technology, {APCST2015}.
[14] M. Damsgaard, J. Rasmussen, S. T. Christensen, E. Surma, M. de Zee, Analysis of musculoskeletal systems in the anybody modeling system, Simulation Modelling Practice and Theory 14 (2006) 1100 – 1111. {SIMS} 2004.
[15] S. Zeller, T. Abel, Auswirkungen nicht zirkulärer Kettenblätter auf physiologische Parameter im Handcyclesport, BISp-Jahrbuch Forschungsförderung 2010/11 (2010).
[16] A. Faupin, P. Gorce, E. Watelain, C. Meyer, A. Thevenon, A biomechanical analysis of handcycling: a case study, Journal of applied biomechanics 26 (2010) 240–245.